PLOS ONE

RESEARCH ARTICLE

Effect of CO_2-induced seawater acidification on growth, photosynthesis and inorganic carbon acquisition of the harmful bloom-forming marine microalga, *Karenia mikimotoi*

Shunxin Hu☯, Bin Zhou☯, You Wang, Ying Wang, Xinxin Zhang, Yan Zhao, Xinyu Zhao, Xuexi Tang*

Department of Marine Ecology, College of Marine Life Sciences, Ocean University of China, Qingdao, China

☯ These authors contributed equally to this work.
* tangxx@ouc.edu.cn

Citation: Hu S, Zhou B, Wang Y, Wang Y, Zhang X, Zhao Y, et al. (2017) Effect of CO_2-induced seawater acidification on growth, photosynthesis and inorganic carbon acquisition of the harmful bloom-forming marine microalga, *Karenia mikimotoi*. PLoS ONE 12(8): e0183289. https://doi.org/10.1371/journal.pone.0183289

Editor: Hans G. Dam, University of Connecticut, UNITED STATES

Received: July 14, 2016

Accepted: August 2, 2017

Published: August 16, 2017

Data Availability Statement: All relevant data are within the paper.

Funding: This work was supported by the Natural Science Foundation of China (41476091) and NSFC-Shangdong Joint Fund (U1406403).

Competing interests: The authors have declared that no competing interests exist.

Abstract

Karenia mikimotoi is a widespread, toxic and non-calcifying dinoflagellate, which can release and produce ichthyotoxins and hemolytic toxins affecting the food web within the area of its bloom. Shifts in the physiological characteristics of *K. mikimotoi* due to CO_2-induced seawater acidification could alter the occurrence, severity and impacts of harmful algal blooms (HABs). Here, we investigated the effects of elevated pCO_2 on the physiology of *K. mikimotoi*. Using semi-continuous cultures under controlled laboratory conditions, growth, photosynthesis and inorganic carbon acquisition were determined over 4–6 week incubations at ambient (390ppmv) and elevated pCO_2 levels (1000 *ppmv* and 2000 *ppmv*). pH-drift and inhibitor-experiments suggested that *K. mikimotoi* was capable of acquiring HCO_3^-, and that the utilization of HCO_3^- was predominantly mediated by anion-exchange proteins, but that HCO_3^- dehydration catalyzed by external carbonic anhydrase (CA_{ext}) only played a minor role in *K. mikimotoi*. Even though down-regulated CO_2 concentrating mechanisms (CCMs) and enhanced gross photosynthetic O_2 evolution were observed under 1000 ppmv CO_2 conditions, the saved energy did not stimulate growth of *K. mikimotoi* under 1000 ppmv CO_2, probably due to the increased dark respiration. However, significantly higher growth and photosynthesis [in terms of photosynthetic oxygen evolution, effective quantum Yield (Yield), photosynthetic efficiency (α), light saturation point (E_k) and ribulose-1,5-bisphosphate carboxylase/oxygenase (Rubisco) activity] were observed under 2000 ppmv CO_2 conditions. Furthermore, elevated pCO_2 increased the photo-inhibition rate of photosystem II (β) and non-photochemical quenching (NPQ) at high light. We suggest that the energy saved through the down-regulation of CCMs might lead to the additional light stress and photo-damage. Therefore, the response of this species to elevated CO_2 conditions will be determined by more than regulation and efficiency of CCMs.

Introduction

Ocean acidification refers to the ongoing reduction in the ocean pH over an extended period of time, which is primarily caused by the uptake of anthropogenic CO_2 from the atmosphere [1, 2]. Industrialization and fossil fuel combustion have increased the atmospheric CO_2 concentrations from pre-industrial levels of approximately 280 *ppmv* to the current level of approximately 390 *ppmv* [2, 3]. The atmospheric CO_2 concentrations are predicted to increase to 1000 *ppmv* and 2000 *ppmv* by the years 2100 and 2300, respectively, if the present energy utilization structure persists [1]. Such increases in CO_2 would lead to a reduction in pH (0.4 and 0.77 units, respectively) and cause substantial chemical changes in seawater carbonate systems, including increases in pCO_2, HCO_3^- and DIC and decreases in H^+ and CO_3^{2-} [4, 5].

Marine phytoplankton assimilates inorganic carbon and fixes CO_2 into carbohydrates through the enzyme ribulose-1,5-bisphosphate carboxylase/oxygenase (Rubisco), which can only use CO_2 as substrate for the carboxylase reaction. Rubisco is generally characterized by low affinities for CO_2 (K_M of 20–70 μmol L^{-1}), and a competitive reaction with O_2 further reduces its efficiency [6]. Therefore, photosynthesis of some marine phytoplankton might suffer from CO_2 limitation, due to the present concentration of aqueous CO_2 in seawater ranging from 8 to 20 μmol L^{-1}. Most marine phytoplankton have developed so-called CO_2 concentrating mechanisms (CCMs) to overcome the deficiencies of Rubisco. Two main types of CCMs are suggested to be involved in marine phytoplankton. Firstly, the dehydration of HCO_3^- is catalyzed by external carbonic anhydrase, facilitating the supply of CO_2 at plasma membrane and improving the potential for CO_2 uptake, and then CO_2 accumulation is achieved by the active transport of HCO_3^- or CO_2 at the chloroplast envelope. Secondly, HCO_3^- is transported across the plasmalemma and/or chloroplast envelope and then converted to CO_2, catalyzed by one of several types of internal carbonic anhydrase [7]. However, the expression and operation of CCMs require energetic investment. Therefore, marine phytoplankton could benefit from elevated pCO_2 in two synergetic ways: one is that the increased dissolved carbon dioxide (CO_2aq) would supply additional substrate for photosynthetic carbon fixation and reduce the oxygenase reaction of Rubisco, alleviating the carbon limitations of species without a CCM [8]. The other is that, increased pCO_2 could down-regulate the energetically costly operation of CCMs.

Many marine phytoplankton species down-regulate their operation of CCMs at high pCO_2 conditions, as revealed by a lower photosynthetic affinity for CO_2, decreased activities of carbonic anhydrase and/or a lower contribution of HCO_3^-assimilation [9–12]. This is taken as evidence that elevated pCO_2 exerts positive effects on the growth and photosynthesis of species bearing CCMs[9, 13–15]. Some species (*Macrocystis pyrifera* and *Gracilaria lemaneiformis*), however, do not show any deactivation of CCMs or changes in growth and photosynthesis in response to elevated pCO_2 [16, 17]. In addition, increased pCO_2 might exert negative effects on calcifying species because of a lowering of saturation of $CaCO_3$, which might make calcfication more difficult [18,19]. Deleterious effects of elevated pCO_2, however, also occur on non-calcifying species [20–23], probably due to the negative effects on physiological processes caused by reduced external pH. [24]. Altogether, these findings havedeepened our understandings of differential physiological responses to elevated pCO_2 among various marine phytoplankton species, such as diatoms and coccolithophores.

Karenia mikimotoi is a widespread, toxic and non-calcifying dinoflagellate, which can have deleterious effects on other marine phytoplankton, fish and shellfish through the release of ichthyotoxins and hemolytic toxins [25]. *K. mikimotoi* toxic blooms have been reported in Japan, Ireland, England, France, India and China [26–30]. At least 103 harmful algal blooms (HABs) have been reported between 2004 and 2014 caused by *K. mikimotoi* in eastern and southern Chinese seas, affecting about 37527 km^2 (according to China Marine Disaster

Bulletin). Owing to its ecological and environmental implications, it is necessary to study the physiological responses of this species to elevated pCO_2 in order to predict the occurrence, severity and impacts of blooms of this species in the future. In the present study, we evaluated growth, photosynthesis, dark respiration and the CCMs modes of *K. mikimotoi* exposed to three different pCO_2 levels: 390 *ppmv* (pH_{NBS}: 8.10) which is the present pH value, as well as 1000 *ppmv* (pH_{NBS}: 7.78) and pCO_2: 2000 *ppmv* (pH_{NBS}: 7.49), which are predicted to be possible conditions in 2100 and 2300, respectively. We hypothesized that (1) the operation of CCMs will be down-regulated with elevated pCO_2 and (2) the reduction in the energy costs of CCMs will benefit growth and photosynthesis of *K. mikimotoi*.

Materials and methods

Culture conditions and experimental design

Karenia mikimotoi (strain OUC151001) was obtained from the Algal Culture Collection at the Ocean University of China. Cells were cultured in 0.45μm-filtered natural seawater, collected from Luxun Seaside Park (Qingdao), which had been autoclaved (30min, 121˚C) and enriched with f/2 medium [31]. All cultures were incubated at 20±1˚C and illuminated with 80 μmol photon m^{-2} s^{-1} under a 12:12 light: dark cycle.

Experiments were conducted in triplicate 1000 ml sterilized and acid-washed Erlenmeyer flask containing 600 ml of medium. Prior to inoculation, the cultures were equilibrated at three different CO_2 levels: 390 *ppmv* CO_2 (~present-day), 1000 and 2000 *ppmv* CO_2 (predicted CO_2 levels in 2100 and 2300, respectively), obtained by gentle bubbling with 0.22 μm-filtered ambient air and air/CO_2 mixtures. The air/CO_2 mixtures were generated by plant CO_2 chambers (HP400G-D, Ruihua Instrument & Equipment Ltd, Wuhan, China) with a variation of less than 5%. Semi-continuous cultures were used to measure the effects of CO_2-induced seawater acidification on the growth and physiology of *K. mikimotoi* in the present study, similar to previous ocean acidification research [9, 32–34]. All cultures were diluted to 800 cells mL^{-1} with fresh medium pre-acclimated to the desired CO_2 level every 24h to maintain cells in exponential growth phase, and to minimize pH fluctuations. Cultures were harvested following 4–6 weeks of semi-continuous incubation when the growth rates were not significantly different for three or more consecutive days, which was considered fully acclimated to their respective experimental treatments.

Seawater carbonate chemistry

The pH value and dissolved inorganic carbon (DIC) were determined prior to and after the daily dilution. The concentration of DIC in the culture medium was measured using a total organic carbon analyzer (TOC-V_{CPN}, Shimadzu). The samples were filtered onto brown glasses via 0.45 μm cellulose acetate membranes and stored in a refrigerator (4˚C). The pH was measured using a pH meter (SevenCompact™ S210k, Mettler Toledo, Switzerland), which was calibrated daily with standard National Bureau of Standards (NBS) buffer system. The other relevant parameters of carbonate system were determined with the CO_2SYS software [35], based on the known parameters (pH, DIC, salinity and temperature).

Growth and elemental analysis

Cell growth rate was monitored daily using a plankton counting chamber (0.1 mL) before and after the medium was diluted. The specific growth rate (μ) was calculated using the equation:

$$\mu = (\ln N_1 - \ln N_0)/(t_1 - t_0),$$

where N_0 and N_1 represent the average cell numbers at times t_0 (after the dilution) and t_1 (before the dilution), respectively.

Samples for measurements of cellular carbon (C), nitrogen (N) and phosphorus (P) were filtered onto glass microfiber membranes (GF/F, Whatman), which were pre-combusted at 500˚C for 4 h, and then stored at -20˚C in a refrigerator before analysis. Cellular C and N content were determined using a Perkin-Elmer 2400 CHNS analyzer following the method of Zhao et al. [36]. Cellular P content was measured as in Fourqurean et al. [37].

Chlorophyll *a*

Chlorophyll *a* (Chl *a*) samples from the cultures were filtered onto glass microfiber filters (GF/F, Whatman), and extracted with 10 mL of methanol overnight at 4˚C. Samples were then analyzed in a spectrophotomer, and the Chl *a* concentration was calculated according to the following equation [38]:

$$\text{Chl a} = 16.29 \times (A_{665} - A_{750}) - 8.54 \times (A_{652} - A_{750})$$

where A_{652}, A_{665} and A_{750} denoted the absorbance values of the methanol extracts at 652nm, 665nm and 750nm, respectively.

Photosynthetic oxygen evolution and respiration

Photosynthetic oxygen evolution was measured under the same light intensities used for growing cultures, with lighting provided by a halogen lamp. The dark respiration rate was determined using a Clark-type oxygen electrode (Chlorolab 3, Hansatech, UK). Experimental temperature was maintained at 20˚C using a water bath circulator. Before the determination, cells were acclimated to light or dark conditions in the reaction chamber for 20 min. The 5ml-reaction media was continuously stirred with a magnetic stirrer during treatment. DIC concentrations were consistent with their culture conditions, which were nominally 390ppmv: 1919–1924 μmol/kg; 1000ppmv: 2059–2067 μmol/kg; 2000 ppmv:2152–2156 μmol/kg, respectively.

Chlorophyll fluorescence measurements

Fluorescence induction curves and rapid light curves (RLCs) were applied to evaluate the photosynthetic performance of *K. mikimotoi* acclimated to different pCO_2, using a Water-PAM fluorometer.

The RLCs were measured at 8 different actinic irradiance levels (80, 119, 184, 276, 393, 546, 897 and 1315 μmol photon m^{-2} s^{-1}), each of which lasted 10s. To quantitatively compare the RLCs of *K. mikimotoi* acclimated to different pCO_2, the equation of Platt et al. [39] was applied to derive characteristic parameters: photosynthetic efficiency (α), light saturation point (E_k), photo-inhibition rate of photosystemII(β) and maximum relative electron transport rate ($rETR_{max}$). The light saturation point was determined from: $E_k = rETR_{max}/\alpha$ [40]. Related parameters were applied to determine the convergence of the regression mode according to Ralph and Gademann [40].

For the fluorescence induction curves, all of the samples were dark-acclimated for 20 mins before determination. The dark-acclimation induction curves were measured with a delay of 40 s between the determinations of F_v / F_m. The actinic light was set at 80, 276 and 897 μmol photon m^{-2} s^{-1}, respectively, to measure the value of effective quantum yield (Yield) and non-photochemical quenching (NPQ)

Determination of ribulose-1,5-bisphosphate carboxylase/oxygenase (Rubisco) activities

Cells were collected by centrifugation at a rotating speed of 3000g at 4˚C for 15 min. After removing the supernatant, cells were grinded on ice with the addition of 1mL buffer solution (40 mM Tris-HCl, 5 mM Glutathione, 10 mM $MgCl_2$ and 0.25 mM EDTA, pH 7.6). The liquid was concentrated, and the supernatant was used for further assays. Rubisco activity in the supernatant was generally determined following the methods described by Gerard and Driscoll [41]. The assay mixture contained 5 mM NADH, 50 mM ATP, 50 mM phosphocreatine, 0.2 mM $NaHCO_3$, 160 U/mL creatine phosphokinase, 160 U/mL Phosphoglycerate kinase, 160 U/mL glyceraldehyde-3-phosphate dehydrogenase and reaction buffer (0.1M Tris-HCl, 12 mM $MgCl_2$ and 0.4 mM EDTA, pH 7.8). Absorbance values at 340 nm (A_{340}) were measured every 20s for 3 min to obtain the background NADH oxidation rate. A volume of 0.05 mL of RuBP (final concentrations of 25 mM) was added into the assay mixture, and the A_{340} was then recorded every 20 s for 3 min. The activities of Rubisco were computed by subtracting the background rate of decrease in A_{340} from the rate determined during the three minutes following RuBP addition, and then converting the corrected rate of A_{340} decrease to a rate of NADH oxidation.

pH drift experiment

A pH drift experiment was applied to determine whether *K. mikimotoi* can utilize HCO_3^- as an inorganic carbon source; the ability of algae to raise the medium pH to higher than 9.0 is considered as evidence of its capacity to utilize HCO_3^-. The experiment was performed in sterilized glasses containing 10 mL samples (cell concentrations of 10×10^4 mL^{-1}) at 20˚C and 80 μmol photon m^{-2} s^{-1}. The pH was measured every hour and the final pH values were obtained once no further pH increases were detected.

Determination of carbonic anhydrase activity

Cells were collected by centrifugation at a rotating speed of 3000g at 4˚C for 15 min and re-suspended in 20mM barbitone (pH 8.2). The total carbonic anhydrase (CA_{tot}) and external carbonic anhydrase (CA_{ext}) activities were measured using an electrometric method [42]. For determination of CA_{tot}, cells were disrupted with a sonicator, and cell brakage confirmed under a microscope. The reaction was begun by adding 2 mL ice-cold CO_2 to saturated Milli-Q water, and the time it took for the pH to decrease from 8.2 to 7.2 was recorded. The temperature was controlled at 4˚C.

Effect of inhibitors on chlorophyll fluorescence

The RLCs of *K. mikimotoi* acclimated to different pCO_2 with addition of inhibitors were obtained to determine the mechanism of inorganic carbon acquisition. The inhibitors included acetazolamide (AZ), which inhibits only extracellular CA, ethoxyzolamide (EZ), which inhibits both extracellular and intracellular CA, and DIDS (4,4'-diisothiocyanostilbene-2,2'-disulfonate), which inhibits direct HCO_3^- uptake by means of the anion-exchange protein. These inhibitors have been widely used to determine the contribution of external CA, internal CA and anion-exchange protein to photosynthetic inorganic carbon uptake [21, 43, 44].

Statistical analysis

One-way ANOVA was used to analyze the significance of the differences between treatments using the SPSS software (20.0), and the significant difference level was set to $P < 0.05$. All figures were prepared with Sigmaplot 12.5.

Results

Seawater carbonate chemistry

Under the simulated laboratory conditions of ocean acidification, the seawater carbonates chemistry system at elevated pCO_2 (1000 *ppmv* and 2000 *ppmv*) levels significantly differed from that of the control group (Table 1). The DIC, CO_2 and HCO_3^- concentrations in the 1000 *ppmv*-treated system were increased by 7.0%, 125.9% and 10.1%, respectively, whereas in the 2000 *ppmv*-treated system, these values increased by 12.1%, 361.4% and 15.5%, respectively. The CO_3^{2-} concentrations were decreased by 46.5% and 71.1% in the 1000 *ppmv*- and 2000 *ppmv*-treated systems, respectively, and the difference in total alkalinity (TA) was insignificant. The fluctuations of pH prior and after the dilution of the culture medium were <0.03.

Growth and elemental composition

The growth rates at the three pCO_2 levels are shown in Fig 1. The growth rate of *K. mikimotoi* was significantly stimulated by 16.84% ($P<0.05$) after exposure to 2000 *ppmv* pCO_2; although growth was also enhanced under 1000 *ppmv* pCO_2, the increase was not statistically significant ($P>0.05$).

The total cellular C,N,P and their elemental ratio in *K. mikimotoi* are shown in Table 2. The cellular C and P concentrations of *K. mikimotoi* exposed to 2000 *ppmv* pCO_2 levels were significantly ($P<0.05$) higher than those of the control, whereas there was no significant difference between the control and 1000 *ppmv* pCO_2 ($P>0.05$). Furthermore, elevated pCO_2 exerted no significant effects on the cellular N, C: N, C: P and N: P ratios ($P>0.05$).

Chlorophyll *a*

Cells acclimated to the three pCO_2 levels showed the same Chl *a* content (Fig 2) of about 2.0 pg $cell^{-1}$, with no significant differences among treatments.

Photosynthetic oxygen evolution, dark respiration and Rubisco activities

Results of the determinations of the net photosynthetic oxygen evolution, gross photosynthetic oxygen evolution, dark respiration, and Rubisco activity are shown in Fig 3. Net photosynthetic oxygen evolution (Fig 3A) and Rubisco activity (Fig 3D) were significantly enhanced by 22.86% ($P<0.05$) and 31.99% ($P<0.05$) under 2000 *ppmv* pCO_2, whereas there were no significant difference between the control and 1000 *ppmv* pCO_2 ($P>0.05$). Cells acclimated to both 1000 *ppmv* and 2000 *ppmv* pCO_2 treatments showed higher gross photosynthetic oxygen evolution (Fig 3B) and dark respiration (Fig 3C) than those of the control ($P<0.05$).

Table 1. Parameters of the seawater carbonate chemistry system at different pCO_2 levels prior and after the dilution. The dissolved inorganic carbon (DIC) concentration, pH_{NBS}, temperature and salinity were used to compute other parameters with a CO_2 system analyzing software (CO_2SYS). Data are shown as the mean ± SE (n = 9). Different letters represent significant difference between variables (P < 0.05).

		pH_{NBS}	DIC/(μmol/kg)	HCO_3^-/(μmol/kg)	CO_3^{2-}/(μmol/kg)	CO_2/(μmol/kg)	TA/(μmol/kg)
Control	Prior	8.13±0.02[a]	1919.6±9.0 [a]	1762.8±4.0 [a]	142.3±5.4 [a]	14.4±1.4 [a]	2113.6±16.9 [a]
	After	8.10±0.02[a]	1924.6±14.7 [a]	1773.9±12.6 [a]	135.2±2.3 [a]	15.4±1.2 [a]	2110.9±17.3 [a]
1000*ppmv*	Prior	7.81±0.01[b]	2067.7±14.3[b]	1957.7±12.6 [b]	75.5±2.4 [b]	33.6±0.6 [b]	2143.9±18.0 [a]
	After	7.78±0.02 [b]	2059.6±14.2 [b]	1951.6±12.7 [b]	72.4±2.0 [b]	34.8±0.5 [b]	2131.9±17.3 [a]
2000*ppmv*	Prior	7.52±0.01[c]	2152.6±11.6 [c]	2053.3±24.0 [c]	41.2±1.3 [c]	67.7±0.8 [c]	2145.9±13.1 [a]
	After	7.50±0.02 [c]	2156.3±14.6 [c]	2048.7±9.8 [c]	39.1±1.3 [c]	71.0±1.6 [c]	2141.1±14.0 [a]

https://doi.org/10.1371/journal.pone.0183289.t001

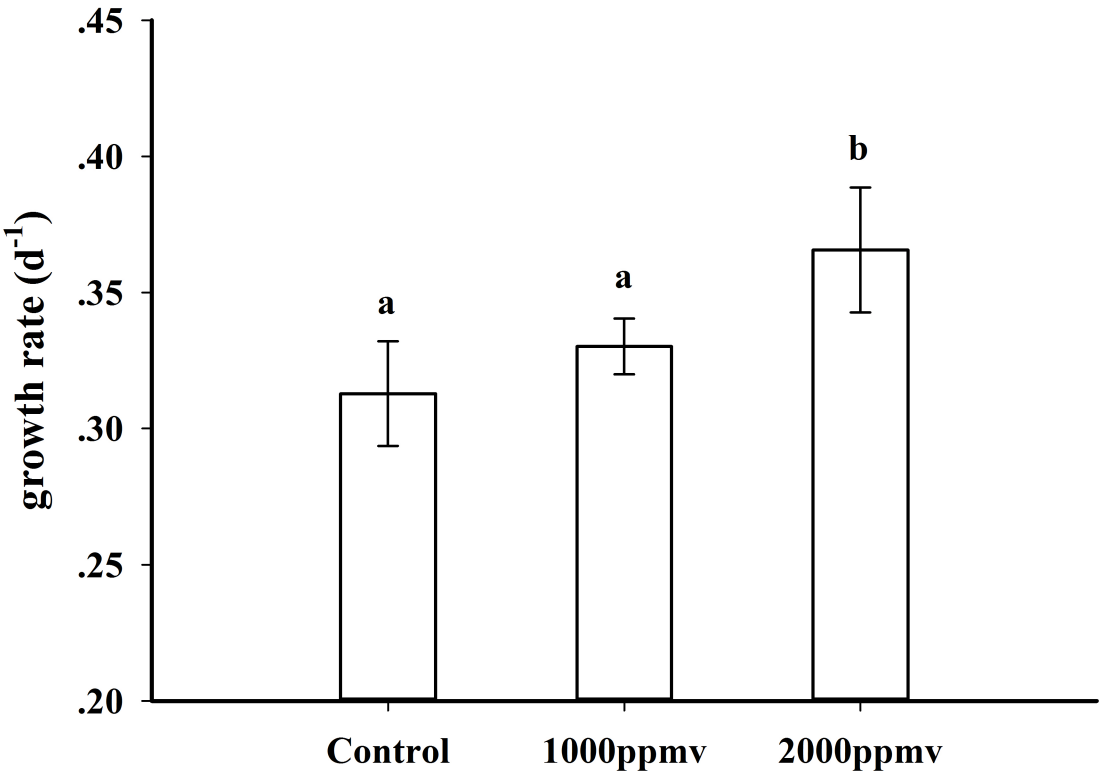

Fig 1. Growth rate of *K. mikimotoi* acclimated to different pCO_2 levels. Data are shown as the mean ± SE (n = 9).

https://doi.org/10.1371/journal.pone.0183289.g001

Chlorophyll fluorescence

Rapid light curves (RLCs) were determined at the three levels of pCO_2 (control, 1000 *ppmv* and 2000 *ppmv*). The three treatments all exhibited a classical pattern of rETR as a function of PAR (Fig 4A), with a rapid increase under light-limited conditions followed by a plateau, at which the photosynthetic pathway was saturated.

The parameters derived from the RLCs are shown in Table 3. The photosynthetic efficiency (α) of *K. mikimotoi* was significantly stimulated by 23.1% ($P<0.05$) under 2000 *ppmv* pCO_2. Cells acclimated to 1000 *ppmv* pCO_2 also showed higher α than that of control, but the increase was not statistically significant ($P>0.05$). Contrary to the trend observed in α, elevated pCO_2 significantly decreased the light saturation point (E_k) of *K. mikimotoi* by 7.5% ($P<0.05$) and 10.2% ($P<0.05$) under 1000 and 2000 *ppmv* CO_2 compared with the control, respectively. The maximum relative electron transport rates ($rETR_{max}$) were approximately 10% higher in both elevated pCO_2 levels compared with the control, but the differences were not significant ($P > 0.05$). Moreover, the results showed that increased pCO_2 levels had no significant effect on the F_v / F_m of *K. mikimotoi* ($P > 0.05$).

The inhibition of rETR was obtained from the rapid light curves in all three different pCO_2 levels when exposed to the actinic irradiance of 1315 μmol photon m^{-2} s^{-1}. β values (relative inhibition), characterizing the photo-inhibition rate of PSII exposed to high actinic irradiance, were significantly increased by 126.7% ($P<0.01$) and 194.3% ($P<0.001$), respectively, in 1000 *ppmv* and 2000 *ppmv* pCO_2 compared with the control (Table 3).

The non-photochemical quenching (NPQ) and effective quantum yield of PS II (Yield) values derived from the induction light curve (IC) are shown in Figs 5 and 6, respectively. The

Table 2. Elemental composition (total C, N and P) and elemental ratio (C:N, C:P and N:P) of *K. mikimotoi* acclimated to different pCO_2 levels. Data are shown as the mean ± SE (n = 9). Different letters represent significant difference between variables (P < 0.05).

pCO_2	C pmol cell^{-1}	N pmol cell^{-1}	P pmol cell^{-1}	C:N	C:P	N:P
Control	6.43±0.70^{a}	1.23±0.07^{a}	0.082±0.007^{a}	5.27±0.85^{a}	78.2±2.8^{a}	15.09±2.36^{a}
1000 *ppmv*	7.63±0.46^{ab}	1.33±0.03 ^{a}	0.081±0.004 ^{a}	5.72±0.23^{a}	93.9±9.9^{a}	16.39±1.14^{a}
2000 *ppmv*	7.99±0.36^{b}	1.34±0.11 ^{a}	0.093±0.003^{b}	5.96±0.32^{a}	85.2±7.2^{a}	14.29±0.92^{a}

https://doi.org/10.1371/journal.pone.0183289.t002

results indicated that response of NPQ to higher CO_2 concentrations depended on actinic irradiances. Under 80 μmol photon m^{-2} s^{-1}, the NPQ values in the 390*ppmv* pCO_2 were 15.4% (P<0.05) and 43.9% (P<0.01) higher than those observed in the 1000 *ppmv* and 2000 *ppmv* pCO_2, respectively. By contrast, NPQ values at 276 and 897 μmol photon m^{-2} s^{-1} were significantly increased in the two high pCO_2 groups ($P < 0.01$), but there was no significant difference between 1000 *ppmv* and the control when exposed to 276 μmol photon m^{-2} s^{-1} (P>0.05). Relative to the control conditions, both the 1000 *ppmv* and 2000 *ppmv* pCO_2 groups significantly stimulated the Yield, which was increased by 4.0% (P<0.05) and 4.9% (P<0.01) at 80 μmol photon m^{-2} s^{-1}, and increased by 11.8% (P<0.05) and 11.8% (P<0.05) at 897 μmol photon m^{-2} s^{-1}.

At an actinic of 276 μmol photon m^{-2} s^{-1}, the 2000 *ppmv* pCO_2 groups exhibited a significant (P<0.01) increase, but not the 1000 *ppmv* pCO_2 groups.

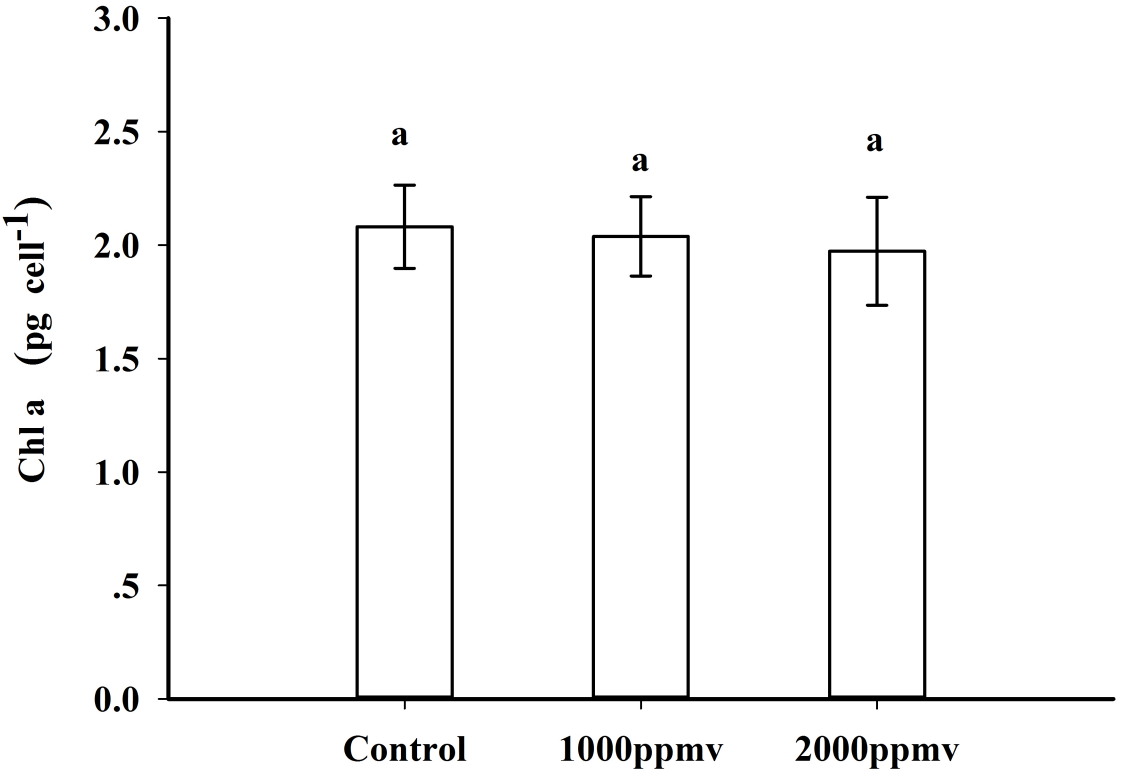

Fig 2. Chlorophyll *a* content of *K. mikimotoi* acclimated to different pCO_2 levels. Data are shown as the mean ± SE (n = 9).

https://doi.org/10.1371/journal.pone.0183289.g002

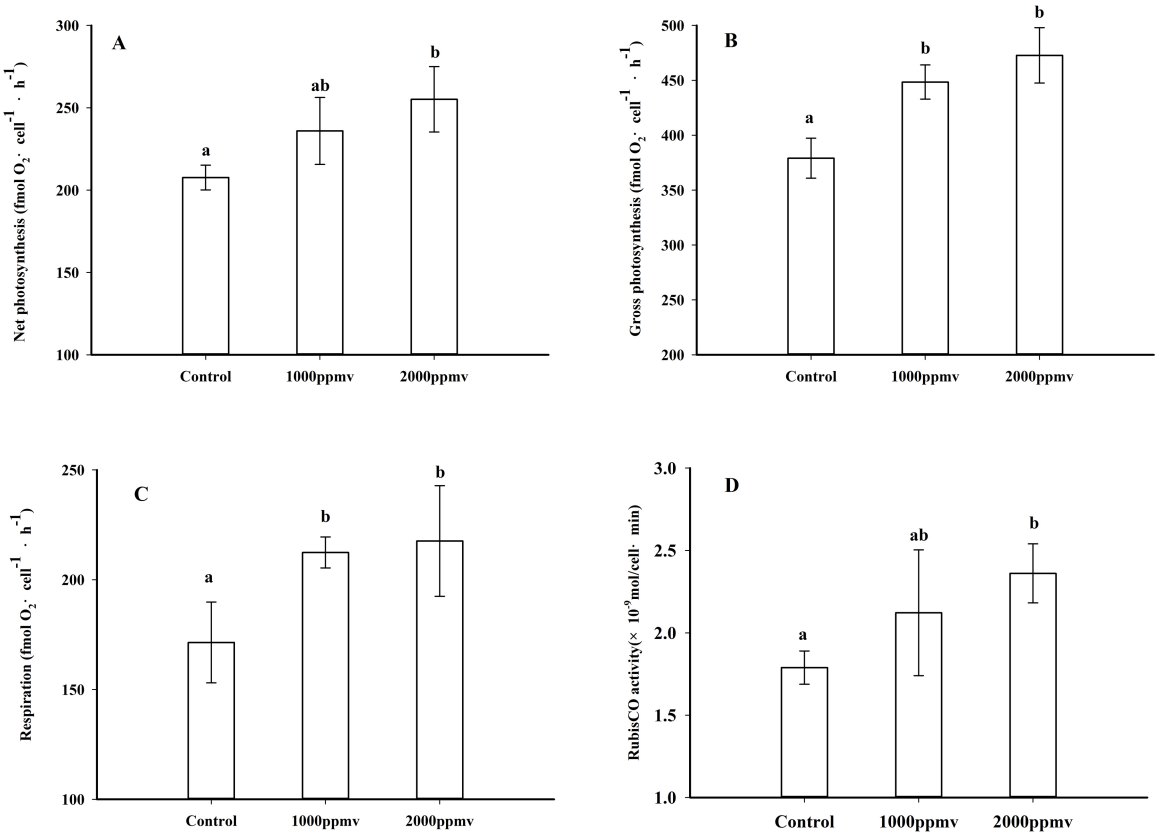

Fig 3. Net photosynthetic oxygen evolution (A), gross photosynthetic oxygen evolution (B), dark respiration (C) and Rubisco activity (D) of *K. mikimotoi* acclimated to different pCO_2 levels. Data are shown as the mean ± SE (n = 9).

https://doi.org/10.1371/journal.pone.0183289.g003

pH drift experiment and carbonic anhydrase activity

The final pH value obtained in the pH drift experiment was 9.8±0.1. Furthermore, the total carbonic anhydrase activity (CA_{tot}) and internal anhydrase activity (CA_{int}) (Fig 7) of *K. mikimotoi* were significantly decreased by 50.6% ($P<0.01$) and 55.5% ($P<0.05$) after exposure to 2000 *ppmv* pCO_2, and no significant changes were observed when exposed to 1000 *ppmv* pCO_2 ($P>0.05$). The external carbonic anhydrase activity (CA_{ext}) (Fig 7) of *K. mikimotoi* was significantly lower than the CA_{int}, and no significant changes were observed when exposed to 1000 *ppmv* ($P>0.05$) and 2000 *ppmv* ($P>0.05$) pCO_2.

Effect of inhibitors on chlorophyll fluorescence

The rapid light curves of *K. mikimotoi* acclimated to different pCO_2 levels with and without the addition of AZ, EZ and DIDS are shown in Fig 4. The results indicated that the rETR values of *K. mikimotoi* were significantly inhibited by the addition of EZ and DIDS, whereas the inhibition of rETR by the addition of AZ was significantly less than that obtained with EZ and DIDS.

The inhibition rates of rETR at different pCO_2 levels obtained with the addition of AZ, EZ and DIDS are shown in Table 4. The results indicated that the inhibitions of rETRs by the addition of EZ and DIDS were significantly ($P<0.01$) higher in the controls than those obtained at the high pCO_2 groups (1000 *ppmv* and 2000 *ppmv*). Furthermore, the results from

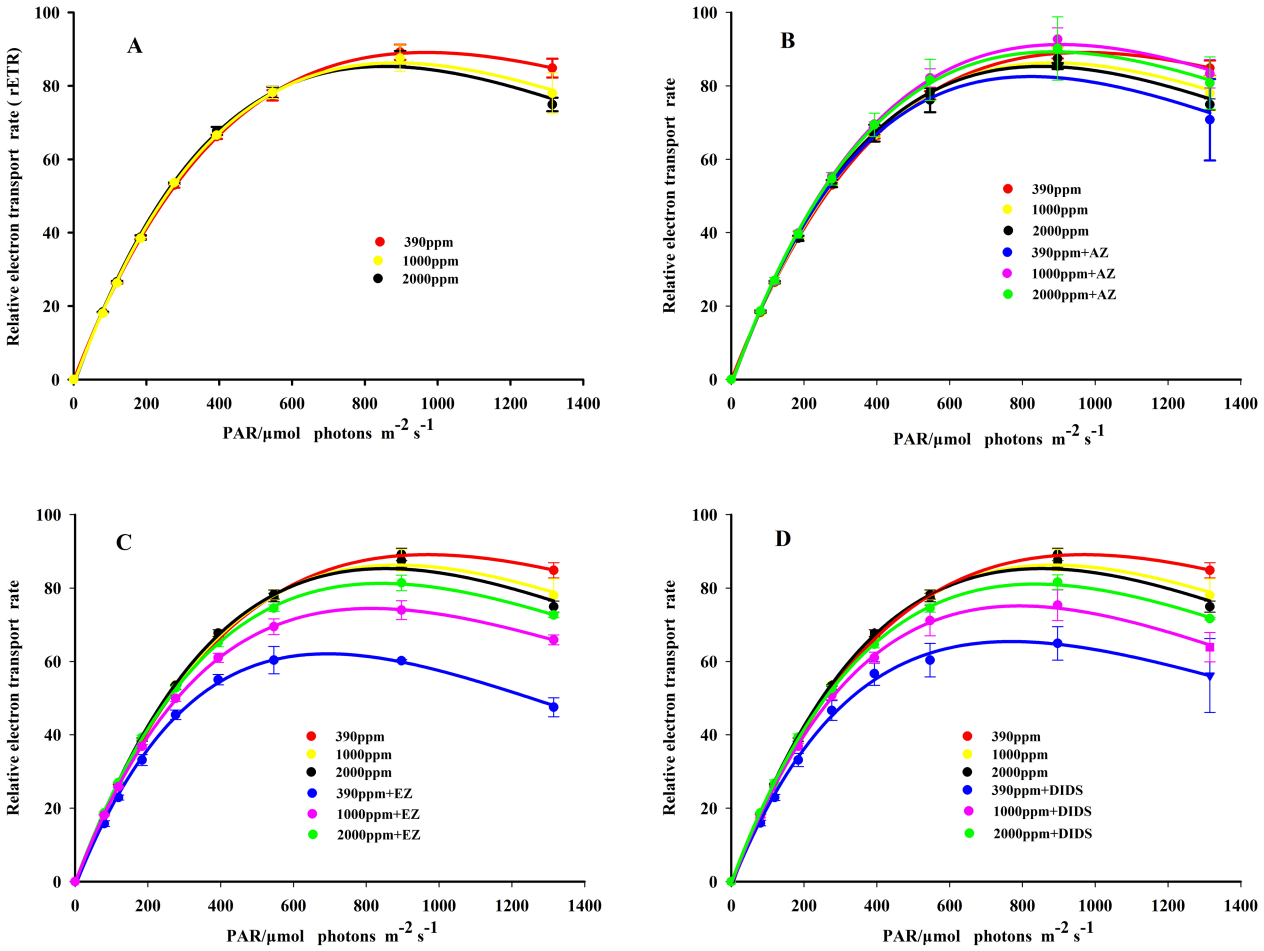

Fig 4. The rapid light curves of *K. mikimotoi* without and with the addition of inhibitors (AZ, EZ and DIDS) acclimated to different pCO_2. Data are shown as the mean ± SE (n = 3).

https://doi.org/10.1371/journal.pone.0183289.g004

all three pCO_2 levels indicated that the inhibition of rETR was significantly increased by the increasing PAR. in the presence of AZ, rETR inhibition was only observed in the 390 *ppmv* pCO_2.

Discussion

Inorganic carbon acquisition

Dinoflagellates are abundant and ecologically important in marine ecosystems, and morphologically and physiologically diverse [45]. They are also the only oxygenic photoautotrophs with type II Rubisco, the enzyme with the lowest affinity for CO_2 among eukaryotic

Table 3. Photosynthetic parameters derived from the rapid light curves of *K. mikimotoi* acclimated to different pCO_2 levels. Data are shown as the mean ± SE (n = 3). Different letters represent significant difference between variables (P < 0.05).

pCO_2	Fv/Fm	A	$rETR_{max}$	E_k	β
390 ppmv	0.599±0.007^a	0.238±0.0150^a	82.8±5.2^a	347.6±5.8^a	0.048±0.007^a
1000 ppmv	0.603±0.008^a	0.285±0.0289^a	91.5±5.5^a	315.7±6.6^b	0.110±0.027^b
2000 ppmv	0.605±0.007^a	0.293±0.0256^b	91.6±10.9^a	312.2±14.9^b	0.143±0.012^b

https://doi.org/10.1371/journal.pone.0183289.t003

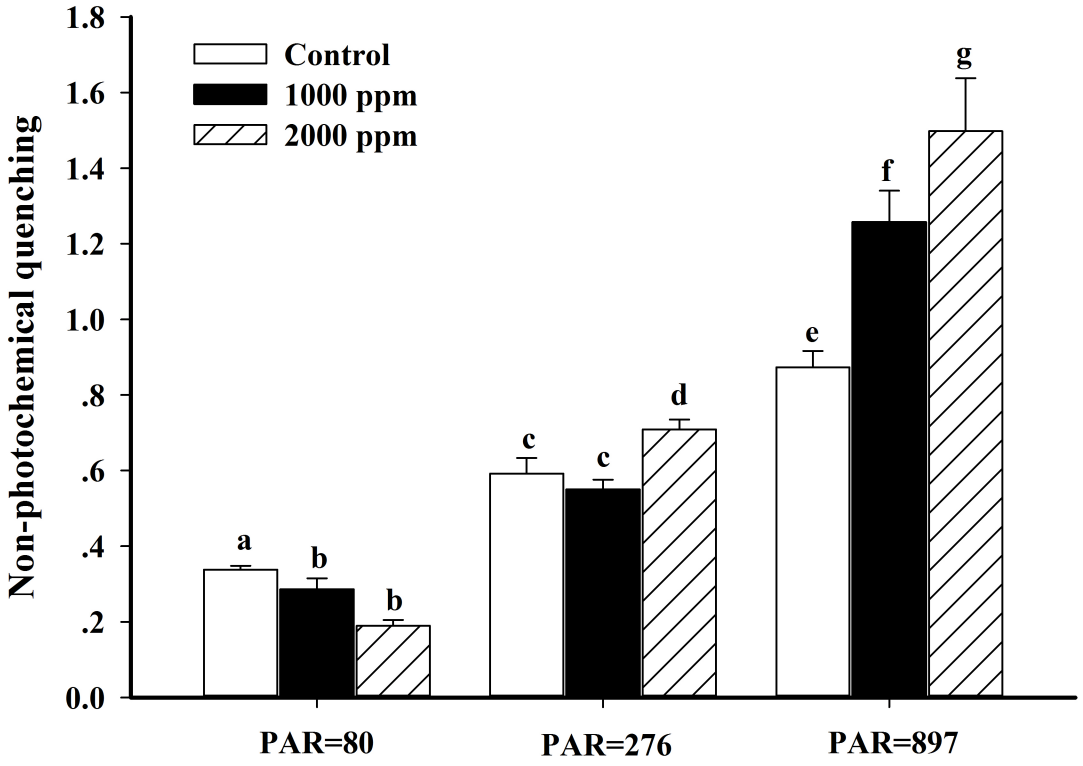

Fig 5. Non-photochemical quenching (NPQ) of *K. mikimotoi* acclimated to different pCO_2 levels at an actinic irradiance of 80, 276 and 897 photon m^{-2} s^{-1}. Data are shown as the mean ± SE (n = 3).

https://doi.org/10.1371/journal.pone.0183289.g005

phytoplankton. Thus, dinoflagellates are at a disadvantage with regard to photosynthetic carbon fixation under the present ocean conditions of low CO_2, and high O_2 [6]. Consequently, dinoflagellates probably require an efficient CCM to compete with other phytoplankton that have higher photosynthetic and growth rates. It is a common notion that the ability of algae to raise the final pH of the medium to higher than 9.0 is an indicator of HCO_3^- utilized by the species [46, 47]. The pH-drift experiments conducted in our study indicated that the final pH value in the medium of *K. mikimotoi* was 9.8±0.1, suggesting that *K. mikimotoi* could use HCO_3^- in seawater. Although most phytoplankton species possess CCMs, large differences exist in their efficiencies. Owing to their rather inefficient CCMs (strongly dependent on CO_2 as inorganic carbon source), the photosynthetic carbon fixation of the coccolithophorid *Emiliania huxleyi* and the raphidophyceae *Heterosigma akashiwo* are well below saturation at present CO_2 levels, and therefore are more CO_2-sensitive than species with highly efficient CCMs (which rely heavily on HCO_3^- as inorganic carbon source), such as *Skeletonema costatum* and *Phaeocystis globose* [32, 48]. In the present study, Rubisco activity of *K. mikimotoi* did not change between 390 and 1000 ppmv, and ETR values only increase slightly (~10%), which is strong evidence that *K. mikimotoi*, similar to *S. costatum* and *P. globose*, relies heavily on HCO_3^- as an inorganic carbon source.

CA_{ext}, which catalyzes the dehydration of HCO_3^- to CO_2 at the cell surface [47–49], was found to decrease at high pCO_2 conditions in other species such as *Phaeocystis globosa* and *S. costatum*, underlining the important role of CA_{ext} in inorganic carbon acquisition [48]. In the present study, such a HCO_3^- dehydration mechanism was likely to contribute very little to the inorganic carbon acquisition in *K. mikimotoi*, because the activities of CA_{ext} were very low in

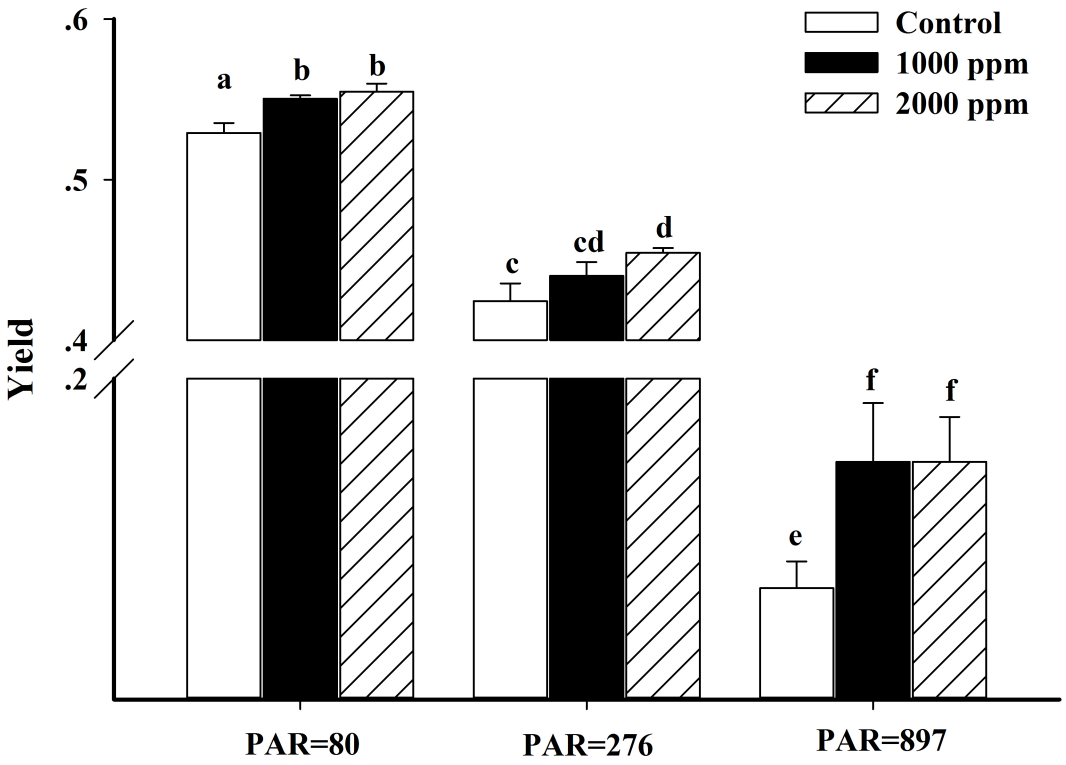

Fig 6. Effective quantum yield (Yield) of *K. mikimotoi* acclimated to different pCO_2 levels at an actinic irradiance 80, 276 and 897 photon m^{-2} s^{-1}. Data are shown as the mean ± SE (n = 3).

https://doi.org/10.1371/journal.pone.0183289.g006

all treatments (Fig 7). Furthermore, the minor role of CA_{ext} was also indicated by the addition of membrane impermeable CA inhibitor AZ, which only slightly inhibited the rETR of *K. mikimotoi* (Fig 4 and Table 4). The low CA_{ext} activity observed in *K. mikimotoi* was consistent with most other tested dinoflagellate species. Rost et al. [50] investigated CA_{ext} activities in *Prorocentrum minimum*, *Heterocapsa triquetra* and *Ceratium lineatum*, and found relatively low or negligible activities in all three species. Eberlein et al. [51] showed that CA_{ext} activities of the dinoflagellate *Alexandrium tamarense* acclimated to a range of pCO_2 from 180 to 1200 μatm were close to detection limits, and thus only played a minor role. However, low CA_{ext} activity is not universal in all dinoflagellate species. High activity of CA_{ext} was found in *Scrippsiella trochoidea*, probably to convert the effluxing CO_2 to HCO_3^-, and then utilized via the HCO_3^- transporter by the cells [51]. This 'CO_2 recirculation mechanism' might be especially beneficial for species with high dark respiration rates.

Furthermore, direct HCO_3^- uptake via the anion-exchange (AE) protein has also been observed in other species, which suggests that HCO_3^- utilization could be inhibited by the AE protein inhibitor, DIDS [52–53]. From our results, such a direct HCO_3^- uptake was likely to be present in *K. mikimotoi*, and it was significantly reduced when the cells acclimated to 1000 and 2000 *ppmv* pCO_2, because the rETR of *K. mikimotoi* was drastically depressed by the addition of DIDS, and the inhibition decreased at high pCO_2 as compared with the control (Fig 4 and Table 4). Down-regulated CCMs at high pCO_2 have also been found in widely distributed species such as *Skeletonema costatum*, *Emiliania huxleyi*, *Thalassionema nitzschioides* and *Pseudo-nitzschia multiseries* [48,54,55]. This down-regulation might result from the increasing diffusive CO_2 uptake at high pCO_2 conditions, since CO_2 uptake is considered to be less

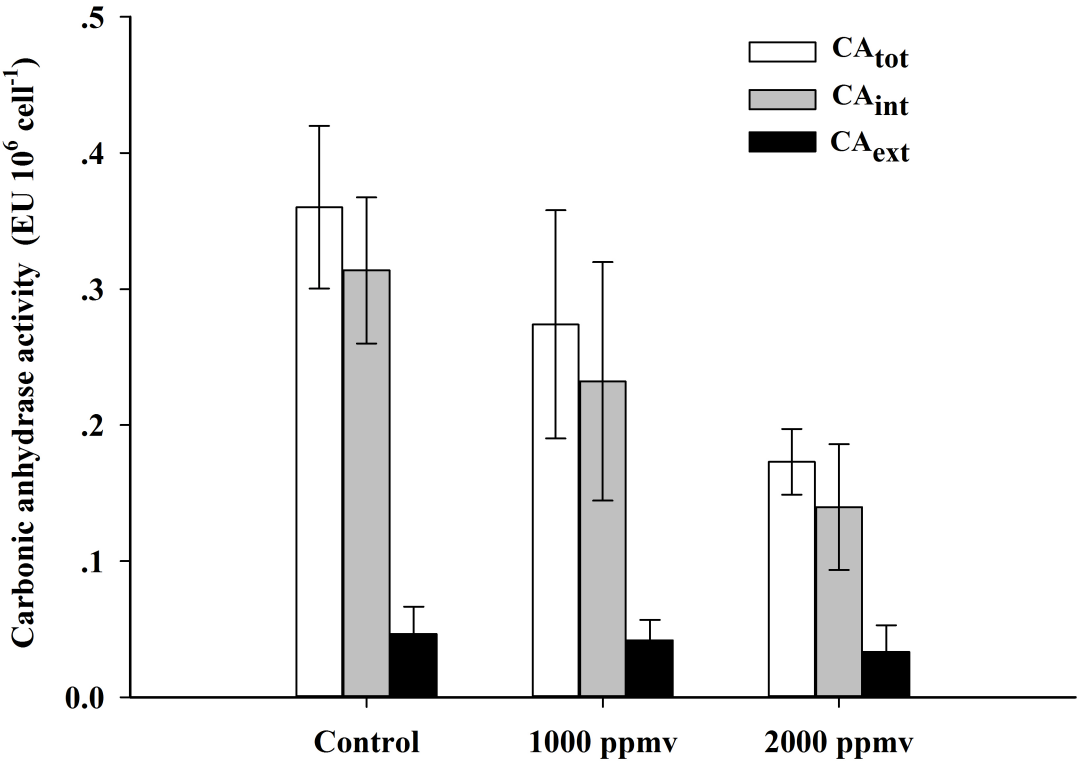

Fig 7. Total, external and internal carbonic anhydrase activity of *K. mikimotoi* acclimated to different pCO_2 levels. Data are shown as the mean ± SE (n = 3).

https://doi.org/10.1371/journal.pone.0183289.g007

Table 4. Percent inhibition of rETR acclimated to different pCO_2 with the addition of AZ, EZ and DIDS within a PAR range of 0 to 1315 μmol photon m^{-2} s^{-1}, "—" represents no inhibition of rETR. Data are shown as the mean ± SE (n = 3).

PAR μmol photon $m^{-2}s^{-1}$	Inhibition rate of rETR								
	390*ppmv* +AZ	1000*ppmv* +AZ	2000*ppmv* +AZ	390*ppmv* +EZ	1000*ppmv* +EZ	2000*ppmv* +EZ	390*ppmv* +DIDS	1000*ppmv* +DIDS	2000*ppmv* +DIDS
80	—	—	—	13.04 ±5.44%	—	—	13.06 ±4.42%	1.30±2.23%	—
119	—	—	—	13.96 ±3.75%	1.65±0.95%	—	13.02 ±3.75%	1.65±0.95%	—
184	0.69 ±3.22%	—	—	14.16 ±5.04%	4.25±1.58%	—	14.44 ±5.04%	4.25±2.20%	—
276	—	—	—	14.46 ±2.10%	6.84±1.35%	1.31±1.17%	11.99 ±4.03%	5.29±1.54%	1.49±0.78%
393	—	—	—	16.87 ±2.12%	8.36±2.13%	3.79±0.52%	14.36 ±4.40%	8.36±2.13%	4.53±0.49%
546	1.68 ±3.54%	—	—	22.04 ±4.47%	11.17 ±5.16%	4.73±0.64%	22.09 ±4.47%	8.94±7.15%	4.72±0.64%
897	4.19 ±1.72%	—	—	32.49 ±1.87%	15.49 ±3.26%	6.94±3.37%	27.09 ±6.49%	13.94±4.47%	7.71±2.78%
1315	9.12 ±1.59%	—	—	43.97 ±2.76%	15.20 ±6.11%	3.07±1.39%	33.98 ±9.98%	17.91±4.97%	4.31±2.79%

https://doi.org/10.1371/journal.pone.0183289.t004

energetically costly than HCO_3^- uptake. Consequently, cells can optimize their allocation of energy and apportion more energy for photosynthetic carbon fixation. Marine phytoplankton productivity based on energy or carbon content might thus increase under typically resource-limited conditions in the ocean. From this point of view, species with regulated CCMs, as shown for *K. mikimotoi*, might have a competitive advantage in the future compared to species that do not react to high pCO_2 such as *Phaeocystis globosa*, *Thalassiosira pseudonana*, *Eucampia zodiacus* and *Nitzschia navis-varingica* [48,54,55]. As a consequence, these different responses of CCMs to elevated pCO_2 might change the fitness of the different group and possibly alter the distribution and succession of marine algae in natural systems.

Growth, photosynthesis, respiration and photosynthetic electron transport

Growth is a comprehensive parameter integrating all physiological processes in marine phytoplankton, and different responses of growth to increased pCO_2 have been reported among different marine phytoplankton species, with positive, negative and no significant responses. According to our experimental results, the growth rate of *K. mikimotoi* was not significantly affected under 1000 ppmv pCO_2 conditions, while the stimulated growth rate was observed under 2000 ppmv pCO_2 conditions. Enhanced growth and photosynthesis by elevated pCO_2 have been reported in species such as the diatoms *Navicula pelliculosa* [56] and *Phaeodactylum tricornutum* [9], the raphidophyceae *Heterosigma akashiwo* [33] and the chlorophyte *Ulva rigida* [57]. However, other studies found no significant effects [32, 58, 59], or even negative effects [22, 60, 61] on the growth, photosynthesis or primary productivity of marine phytoplankton. With regard to the species with highly efficient and strongly regulated CCMs, stimulated growth by elevated pCO_2 is generally attributed to decreased energetic cost of CCMs and HCO_3^- uptake, with the saved energy allocated to support growth [62]. For *K. mikimotoi*, the operation of CCMs were downregulated under both 1000 and 2000 ppmv pCO_2 conditions, but the saved energy from the downregulated CCMs did not stimulate growth under 1000 ppmv pCO_2, probably because of enhanced respiratory carbon loss. Even though gross photosynthesis of *K. mikimotoi* was enhanced under 1000 ppmv pCO_2 (Fig 3B), net photosynthesis was not significantly affected (Fig 3A), which may be largely caused by the enhanced dark respiration. Consequently, the growth of *K. mikimotoi* grown in 1000 ppmv pCO_2 was not significantly stimulated, similarly to what was reported for the diatom *Thalassiosira pseudonana* [10]. When the cells acclimated to 2000 ppmv pCO_2, photosynthesis of *K. mikimotoi* significantly increased. The explanation might be that energy was saved from down-regulation of CCM_S, and thus resulted in increased growth, Results in the present study suggest that the responses of marine phytoplankton to future CO_2-driven seawater acidification are not only determined by the efficiency and regulation of CCMs, but also controlled by the balance of the positive and negative effects associated with increased pCO_2 and seawater acidity.

Enhanced dark respiration rates by elevated pCO_2 have been reported in other species such as the diatom *Thalassiosira pseudonana*, the dinoflagellate *Alexandrium tamarense* and the diatom *Phaeodactylum tricornutum* [9, 10, 52], but not in the dinoflagellate *Scrippsiella trochoidea* and the rhodophyte *Porphyra leucosticte* [51, 63]. Conversely, a decrease in dark respiration was observed in the chlorophyte *Ulva rigida* and the diatom *T. pseudonana* [64, 65]. Stimulation of dark respiration under high pCO_2 condition could reflect higher energy requirement due to either enhanced biosynthesis in response to increased carbon fixation, more energy demand to counteract external pH reduction and to maintain intracellular acid-base stability [66], or pH-dependent changes in the function of respiratory enzymes and altered proton gradient across the mitochondrial membrane [67]. Alternatively, decreased dark respiration by

elevated pCO_2 has been ascribed to the down-regulation of CCMs in order to prevent oxidative damage from excess energy [65].

Comparing the parameters derived from rapid light curves (RLCs) and induction curves, elevated pCO_2 appeared to have a positive impact on the efficiency of PSII, indicated by stimulated α, Yield and decreased E_k at high pCO_2. Generally, photosynthetic efficiency (α) represents the energetic costs of photosynthesis. Accordingly, the present study indicated that future increased pCO_2 reduces the costs of photosynthesis in *K. mikimotoi*. Fu et al. (2007) suggested that a stimulated α at high pCO_2 is attributed to the decreased energetic cost of CCMs and more efficient light use [32]. This suggestion is supported by our findings because the lower contribution of HCO_3^- to inorganic acquisition was also observed in *K. mikimotoi*. The E_k ($rETR_{max}$ / α) represents the optimum light of the photosynthetic apparatus to maintain a balance between photosynthetic energy capture and the capacity to process this energy [68]. For *K. mikimotoi*, an increase in α, and no significant changes in ETR_{max} at high pCO_2 resulted in a decrease in the light saturation point (E_k). This indicates that elevated pCO_2 can stimulate the efficiency of light harvesting and processing of PSII, and thus fewer photons are demanded to reach the E_k at high pCO_2. Furthermore, the lower E_k of *K. mikimotoi* in future CO_2-induced ocean acidification also suggests that light is less likely to be a limiting factor, thus making it more competitive in light-limited conditions. By contrast, the lower E_k also indicated that high pCO_2 lowered the light threshold at which light became excessive in *K. mikimotoi*, and thus the cells easily became photo-inhibited at high light conditions, an inference supported by the increased NPQ (Fig 5) and β (Table 3) at high pCO_2 conditions. The operation of CCMs serves as the pathway for alleviating photo-damage through the dissipation of excess light energy [69, 70]. For *K. mikimotoi*, the more active CCMs in the control would consume more energy and drain more hydrogen ion out of the thylakoid lumen to the stroma, which results in a lower NPQ (Fig 5). Therefore, elevated pCO_2 diminished the energy-dissipation via the down-regulated CCMs, leading to increased NPQ (Fig 5) and enhancing photo-inhibition (Table 3) at high light conditions. Wu et al. (2010) also found that elevated pCO_2 enhanced the photo-inhibition of rETR in *Pheodactylum tricornutum* when exposed to high PAR, but the NPQ decreased at high pCO_2 [9]. In contrast, *Thalsassiosira pseudonana* acclimated to 390 and 1000 ppmv CO_2 showed identical photo-inhibition and NPQ when exposed to high PAR, indicating that high light tolerance was not altered by high pCO_2 [10]. Such different responses among *K. mikimotoi*, *P. tricornutum* and *T. pseudonana* suggest that species-specific metabolic pathways might be involved in coping with elevated pCO_2 and high light stress.

Elemental composition

The elemental composition of marine phytoplankton differs intra and interspecifically. It has been hypothesized that elevated pCO_2 could increase carbon assimilation, and thereby alter the elemental composition of marine phytoplankton. In this study, the similar activities of Rubisco (Fig 3D) and growth rate (Fig 1) under 390 and 1000 ppmv CO_2 treatments suggest that photosynthetic carbon fixation did not differ between these conditions, which could explain why the total cellular carbon, nitrogen and phosphorus contents of *K. mikimotoi* were unaffected by the 1000 ppmv CO_2 conditions. However, the total cellular carbon and phosphorus contents of *K. mikimotoi* increased under 2000 ppmv CO_2, likely due to either enhancement of photosynthetic carbon fixation and elevated uptake of PO_4^{3-}, or to increased activities of phosphatase. Furthermore, enhancement of protein and carbohydrate synthesis also likely contributed to the increased cellular C and P. The unchanged cellular nitrogen contents under 2000 ppmv CO_2 were probably determined by the balance between enhanced nitrogen accumulation and nitrogen loss.

Ecological and environmental implications

It has been proposed that the dominance of bloom-forming species might be dependent on their ability to operate a regulated and efficient CCM [48,54]. In the current study, *K. mikimotoi* was found to have an efficient CCM, and the operation of CCM was down-regulated at high pCO_2 (1000 ppmv and 2000 ppmv) conditions. However, the growth of *K. mikimotoi* in 1000 ppmv pCO_2 was not stimulated by the reduced energetic costs of the CCM, probably due to additional carbon loss caused by enhanced dark respiration. Gao et al. [71] conducted an experiment to investigate the responses of natural phytoplankton assemblages in the South China Sea grown, over a range of light, to elevated pCO_2. The results showed that growth rates of three diatom species (*Thalassiosira pseudonana*, *Phaeodactylum tricornutum*, and *Skeletonema costatum*) under 1000 ppmv pCO_2 were significantly stimulated at low light levels. The different responses between the dinoflagellate *K. mikimotoi* and the diatoms *T. pseudonana*, *P. tricornutum* and *S. costatum* suggest that ongoing CO_2-related changes could affect their dominance and succession in the future, possibly not favoring *K. mikimotoi* in inter-specific competitions.

Global changes not only involve increasing CO_2 levels, but also other environmental factors such as shifts in light availability, nutrient supplies and temperature. Further studies will need to investigate whether species response to elevated pCO_2 might be modulated by other interactive environmental factors. It will be critical to establish the environmental, ecological and economic consequences of *K. mikimotoi* blooms in a future changing ocean.

Acknowledgments

We are thankful to all of the members of the laboratory and Dr. Liang in the College of Fisheries in Ocean University of China for help. This study was supported by the Natural Science Foundation of China (41476091) and NSFC-Shangdong Joint Fund (U1406403)

Author Contributions

Conceptualization: Shunxin Hu.

Formal analysis: Xinxin Zhang.

Funding acquisition: Xuexi Tang.

Methodology: Ying Wang.

Project administration: Xuexi Tang.

Writing – original draft: Shunxin Hu, Bin Zhou, Ying Wang, Xinyu Zhao.

Writing – review & editing: Bin Zhou, You Wang, Yan Zhao, Xuexi Tang.

References

1. Caldeira K, Wickett ME. Oceanography: anthropogenic carbon and ocean pH. Nature. 2003; 425 (6956): 365–365. https://doi.org/10.1038/425365a PMID: 14508477
2. Doney SC, Fabry VJ, Feely RA, Kleypas JA (2009) Ocean acidification: the other CO_2 problem. Mar Sci 1. 2009.
3. Griggs DJ, Noguer M. Climate change 2001: the scientific basis. Contribution of working group I to the third assessment report of the intergovernmental panel on climate change. Weather. 2002; 57(8): 267–269.
4. Gattuso JP, Allemand D, Frankignoulle M. Photosynthesis and calcification at cellular, organismal and community levels in coral reefs: a review on interactions and control by carbonate chemistry. Am Zool. 1999; 39(1): 160–183.

5. Raven J, Ball L, Beardall J, Giordano M, Maberly SC. Algae lacking carbon-concentrating mechanisms. Can J Botany 2005; 83(7): 879–890.
6. Badger MR, Andrews TJ, Whitney SM, Ludwig M, Yellowlees DC, Leggat W, et al. The diversity and coevolution of Rubisco, plastids, pyrenoids, and chloroplast-based CO_2-concentrating mechanisms in algae. Can J Botany.1998; 76(6): 1052–1071.
7. Nimer NA, Iglesias-Rodriguez MD, Merrett MJ. Bicarbonate utilization by marine phytoplankton species. J Phycol.1997; 33(4): 625–631.
8. Raven JA, Giordano M, Beardall J, Maberly SC. Algal evolution in relation to atmospheric CO_2: carboxylases, carbon-concentrating mechanisms and carbon oxidation cycles. Philos T Roy Soc Lon B. 2012; 367(1588): 493–507.
9. Wu Y, Gao K, Riebesell U. CO_2-induced seawater acidification affects physiological performance of the marine diatom *Phaeodactylum tricornutum*. Biogeosciences.2010; 7(9): 2915–2923
10. Yang G, Gao K. Physiological responses of the marine diatom *Thalassiosira pseudonana* to increased pCO_2 and seawater acidity. Mar Environ Res. 2012; 79: 142–151 https://doi.org/10.1016/j.marenvres.2012.06.002 PMID: 22770534
11. Rost B, Riebesell U, Burkhardt S, Sültemeyer D. Carbon acquisition of bloom-forming marine phytoplankton. Limnol Oceanogr. 2003; 48(1): 55–67.
12. Kranz SA, Dieter S, Richter KU, Rost B. Carbon acquisition by *Trichodesmium*: the effect of pCO_2 and diurnal changes. Limnol Oceanogr. 2009; 54(2): 548–559.
13. Kim JM, Lee K, Shin K, Kang J H, Lee HW, Kim M, et al. The effect of seawater CO_2 concentration on growth of a natural phytoplankton assemblage in a controlled mesocosm experiment. Limnol oceanogr.2006; 51(4): 1629–1636.
14. Olischläger M, Bartsch I, Gutow L, Wiencke C. Effects of ocean acidification on different life-cycle stages of the kelp *Laminaria hyperborea* (Phaeophyceae) Bot Mar. 2012; 55(5): 511–525.
15. Olischläger M, Bartsch I, Gutow L, Wiencke C. Effects of ocean acidification on growth and physiology of *Ulva lactuca* (Chlorophyta) in a rockpool-scenario. Phycol Res. 2013; 61(3): 180–190.
16. Zou D, Gao K. Effects of elevated CO_2 on the red seaweed *Gracilaria lemaneiformis* (Gigartinales, Rhodophyta) grown at different irradiance levels. Phycologia. 2009; 48(6):510–517.
17. Fernández P A, Roleda M Y, Hurd C L. Effects of ocean acidification on the photosynthetic performance, carbonic anhydrase activity and growth of the giant kelp *Macrocystis pyrifera*. Photosynth Res. 2015; 124(3):293–304. https://doi.org/10.1007/s11120-015-0138-5 PMID: 25869634
18. Kurihara H, Asai T, Kato S, Ishimatsu A. Effects of elevated pCO_2 on early development in the mussel *Mytilus galloprovincialis*. *Aquat. Biol.* 2008; 4(3): 225–233.
19. Van de Waal DB, John U, Ziveri P, Reichart G-J, Hoins M, Sluijs A, et al. Ocean Acidification Reduces Growth and Calcification in a Marine Dinoflagellate. Plos one. 2013; 8 (6): e65987. https://doi.org/10.1371/journal.pone.0065987 PMID: 23776586
20. Mercado J M, Javier F, Gordillo L, Niell F X, Figueroa F L. Effects of different levels of CO_2 on photosynthesis and cell components of the red alga *Porphyra leucosticta*. 1999; J Appl Phycol 11(5): 455–461.
21. Ihnken S, Roberts S, Beardall J. Differential responses of growth and photosynthesis in the marine diatom *Chaetoceros muelleri* to CO_2 and light availability. Phycologia. 2011; 50(2): 182–193
22. Gao K, Helbling EW, Häder DP, Hutchins DA. Ocean acidification and marine primary producers under the sun: interactions between CO_2, warming, and solar radiation. Mar. Ecol. Prog. Ser. 2012; 470: 167–189.
23. Torstensson A, Chierici M, Wulff A. The influence of increased temperature and carbon dioxide levels on the benthic/sea ice diatom *Navicula directa*. Polar Biol. 2012; 35(2): 205–214
24. Flynn KJ, Blackford JC, Baird ME, Raven JA, Clark DR. Beardall J, et al. Changes in pH at the exterior surface of plankton with ocean acidification. Nature climate change. 2012; 2(7): 510–513
25. Yang Z B, Hodgkiss I J. Hong Kong's worst "red tide"—causative factors reflected in a phytoplankton study at Port Shelter station in 1998. Harmful Algae. 2004; 3(2):149–161.
26. Tangen K. Blooms of *Gyrodinium aureolum* (Dinophygeae) in North European waters, accompanied by mortality in marine organisms. Sarsia. 1977; 63(2): 123–133.
27. Vanhoutte-Brunier A, Fernand L, Ménesguen A, Lyons S, Gohin F, Cugier P. Modelling the Karenia mikimotoi bloom that occurred in the western English Channel during summer 2003. Ecol Model. 2008; 210(4): 351–376.
28. Raine R, McMahon T. Physical dynamics on the continental shelf off southwestern Ireland and their influence on coastal phytoplankton blooms. Cont Shelf Res. 1998; 18(8): 883–914.

29. Godhe A, Otta S K, Rehnstam-Holm A S, Karunasagar I, Karunasagar I. Polymerase Chain Reaction in Detection of *Gymnodinium mikimotoi* and *Alexandrium minutum* in Field Samples from Southwest India. Mar Biotechnol. 2001; 3(2):152–62. https://doi.org/10.1007/s101260000052 PMID: 14961378

30. Yao W, Li C, Gao J. Red tide plankton along the south coastal area in Zhejiang province. Marine Science Bulletin. 2006; 25(3):87–91.

31. Guillard R R L. Culture of phytoplankton for feeding marine invertebrates. In:Culture of marine invertebrate animals. Springer.1975; 29–60.

32. Fu FX, Warner ME, Zhang Y, Feng Y, Hutchins DA. Effects of increased temperature and CO_2 on photosynthesis, growth, and elemental ratios in marine *Synechococcus* and *Prochlorococcus* (Cyanobacteria) J Phycol. 2007; 43(3): 485–496.

33. Fu F X, Zhang Y, Warner M E, Feng Y, Sun J, Hutchins DA. A comparison of future increased CO_2 and temperature effects on sympatric *Heterosigma akashiwo* and *Prorocentrum minimum*. Harmful Algae. 2008; 7(1): 76–90.

34. Hutchins D A, Fu F X, Zhang Y, Warner M E, Feng Y, Portune K, et al. CO_2 control of *Trichodesmium* N_2 fixation, photosynthesis, growth rates, and elemental ratios: Implications for past, present, and future ocean biogeochemistry. Limnology and Oceanography.2007; 52(4): 1293–1304.

35. Lewis E, Wallace D, Allison LJ. Program developed for CO_2 system calculations. Tennessee: Carbon Dioxide Information Analysis Center, managed by Lockheed Martin Energy Research Corporation for the US Department of Energy,1998.

36. Zhao Y, Wang Y, Quigg A. The 24 hour recovery kinetics from N starvation in *Phaeodactylum tricornutum* and *Emiliania huxleyi*. J phycol. 2015; 51(4): 726–738. https://doi.org/10.1111/jpy.12314 PMID: 26986793

37. Fourqurean J W, Zieman J C, Powell G V N. Phosphorus limitation of primary production in Florida Bay: evidence from C: N: P ratios of the dominant seagrass *Thalassia testudinum*. Limnol Oceanogr. 1992; 37(1): 162–171.

38. Porra R J. The chequered history of the development and use of simultaneous equations for the accurate determination of chlorophylls a and b. Photosynth Res. 2002; 73: 149–156. https://doi.org/10.1023/A:1020470224740 PMID: 16245116

39. Platt T, Gallegos C L, Harrison W G. Photoinhibition of photosynthesis in natural assemblages of marine phytoplankton. J Mar Res. 1980; 38: 687–701.

40. Ralph PJ, Gademann R. Rapid light curves: a powerful tool to assess photosynthetic activity. Aquat Bot. 2005; 82(3): 222–237.

41. Gerard V A, Driscoll T. A spectrophotometric assay for rubisco activity: application to the kelp *laminaria saccharina* and implications for radiometric assays1. J phycol. 1996; 32(5): 880–884

42. Wilbur K M, Anderson N G. Electrometric and colorimetric determination of carbonic anhydrase. J Biol Chem. 1948; 176(1): 147–154. PMID: 18886152

43. Moroney JV, Husic HD, Tolbert NE. Effect of carbonic anhydrase inhibitors on inorganic carbon accumulation by *Chlamydomonas reinhardtii*. Plant Physiol. 1985; 79(1): 177–183. PMID: 16664365

44. Axelsson L, Ryberg H, Beer S. Two modes of bicarbonate utilization in the marine green macroalga *Ulva lactuca*. Plant Cell Environ. 1995; 18(4): 439–445.

45. Raven J A, Johnston A M. Mechanisms of inorganic-carbon acquisition in marine phytoplankton and their implications for the use of other resources. Limnology and Oceanography. 1991; 36(8):1701–1714.

46. Maberly SC. Exogenous sources of inorganic carbon for photosynthesis by marine macroalgae 1. J Phycol. 1999; 26(3): 439–449.

47. Johnston A M, Maberly S C, Raven J A. The acquisition of inorganic carbon by four red macroalgae. Oecologia.1992; 92(3): 317–326. https://doi.org/10.1007/BF00317457 PMID: 28312597

48. Rost B, Riebesell U, Burkhardt S, Sültemeyer D. Carbon Acquisition of Bloom-Forming Marine Phytoplankton. Limnol and Oceanogr. 2003; 48(1):55–67.

49. Mercado J M, Niell F X. Carbonic anhydrase activity and use of HCO_3^- in *Bostrychia scorpioides* (Ceramiales, Rhodophyceae). Eur J Phycol. 1999; 34:13–19

50. Rost B, Richter K U, Riebesell U, Hansen P J. Inorganic carbon acquisition in red tide dinoflagellates. Plant Cell Environ. 2006; 29(5): 810–822. PMID: 17087465

51. Eberlein T, Van de Waal DB, Rost B. Differential effects of ocean acidification on carbon acquisition in two bloom-forming dinoflagellate species. Physiol plantarum. 2014; 151(4): 468–479.

52. Drechsler Z, Sharkia R, Cabantchik Z I, Beer S. Bicarbonate uptake in the marine maxroalga *Ulva sp*. is inhibited by classical probes of anion exchange by red blood cells. Planta. 1993; 191:34–40

53. Larsson C, Axelsson L, Ryberg H, Beer S. Photosynthetic carbon utilization by *Enteromorpha intestinalis* (Chorophyta) form a Swedish rockpool. Eur J Phycol. 1997; 32:49–54

54. Trimborn S, Lundholm N, Thoms S, Richter K U, Krock B, Hansen P J, et al. Inorganic carbon acquisition in potentially toxic and non-toxic diatoms: the effect of pH-induced changes in seawater carbonate chemistry. Physiol Plantarum. 2008; 133(1):92–105.

55. Trimborn S, Wolf-Gladrow D, Richter K U, Rost B. The effect of pCO_2, on carbon acquisition and intracellular assimilation in four marine diatoms. J Exp Mar Biol Ecol. 2009; 376(1):26–36.

56. LOW-DÉCARIE E, Fussmann GF, Bell G. The effect of elevated CO_2 on growth and competition in experimental phytoplankton communities. Global Change Biology. 2011; 17(8): 2525–2535.58.

57. Gordillo F J L, Niell F X, Figueroa F L. Non-photosyntheticenhancement of growth by high CO_2 level in the nitrophilic seaweed *Ulva rigida C. Agardh* (Chlorophyta). Planta.2001; 213:64–70 PMID: 11523657

58. Chen X, Gao K. Effect of CO_2 concentrations on the activity of photosynthetic CO_2 fixation and extracelluar carbonic anhydrase in the marine diatom *Skeletonema costatum*. Chinese Sci Bull. 2003; 48(23): 2616–2620.

59. Nielsen L T, Hallegraeff G M, Wright S W, Hansen P J. Effects of experimental seawater acidification on an estuarine plankton community. Aquat Microb Ecol. 2011; 65(3): 271–285.

60. Gao K, Ruan Z, Villafane V E, Gattuso J P, Helbling E W. Ocean acidification exacerbates the effect of UV radiation on the calcifying phytoplankter *Emiliania huxleyi*. Limnol Oceanogr. 2009; 54(6): 1855–1862.

61. Montechiaro F, Giordano M. Compositional homeostasis of the dinoflagellate *Protoceratium reticulatum* grown at three different pCO_2. J Plant Physiol. 2010; 167(2): 110–113. https://doi.org/10.1016/j.jplph.2009.07.013 PMID: 19740567

62. Beardall J, Giordano M. Ecological implications of microalgal and cyanobacterial CO_2 concentrating mechanisms, and their regulation. Funct Plant Biol. 2002; 29(3): 335–347.

63. Mercado J M, Javier F, Gordillo L, Niell F X, Figueroa F L. Effects of different levels of CO_2 on photosynthesis and cell components of the red alga *Porphyra leucosticta*. J Appl Phycol. 1999; 11(5):455–461.

64. Gordillo F J L, Niell F X, Figueroa F L. Non-photosynthetic enhancement of growth by high CO_2 level in the nitrophilic seaweed *Ulva rigida C. Agardh* (Chlorophyta). Planta. 2001; 213(1):64–70. PMID: 11523657

65. Hennon G M M, Quay P, Morales R, Swanson L M, Armbrust E V. Acclimation conditions modify physiological response of the diatom *Thalassiosira pseudonana* to elevated CO_2 concentrations in a nitrate-limited chemostat. J phycol. 2014; 50(2): 243–253. https://doi.org/10.1111/jpy.12156 PMID: 26988182

66. Geider R, Osborne B A. Respiration and microalgal growth: a review of the quantitative relationship between dark respiration and growth. New Phytologist. 1989; 12(3): 327–341.

67. Amthor J S. Respiration in a future, higher CO_2 world. Plant Cell Environ. 1991; 14:13–20

68. Falkowski P G, Raven J A. Aquatic photosynthesis. Princeton University Press. 2013.

69. Li Q, Canvin DT. Energy Sources for HCO3− and CO_2 Transport in Air-Grown Cells of *Synechococcus* UTEX 625. Plant physiol. 1998; 116(3): 1125–1132. PMID: 9501145

70. Tchernov D, Helman Y, Keren N, Luz B, Ohad I, Reinhold L, et al. Passive entry of CO_2 and its energy-dependent intracellular conversion to HCO3− in *Cyanobacteria* are driven by a photosystem I-generated ΔμH+. Biol Chem. 2001; 276(26): 23450–23455.

71. Gao K, Xu J, Gao G, et al. Rising CO_2 and increased light exposure synergistically reduce marine primary productivity. Nature Climate Change. 2012; 2(7):519–523.